Physics Letters A 524 (2024) 129793

Contents lists available at ScienceDirect

Physics Letters A

journal homepage: www.elsevier.com/locate/pla

Letter

Thermal stability and properties of silicon-germanium nanocrystals

Shao-Bin Qiu [a,*], Dan-Feng Zhu [a], Ding-Nan Deng [a], Jun-Bo Chen [a], Yu-Jun Zhao [b], Xiao-Bao Yang [b]

[a] School of Physics and Electrical Engineering, Jiaying University, Meizhou, 514015, China
[b] Department of Physics, South China University of Technology, Guangzhou, 510640, China

ARTICLE INFO

Communicated by L.M. Woods

ABSTRACT

Using first-principles calculations and ensemble theory, we have calculated the ground-state energy and electronic properties of $Si_xGe_{10-x}H_{16}$ nanocrystals, and analyzed their stability and properties at finite temperatures. We have determined the numerical correspondence between chemical potential and the proportion of element in $Si_xGe_{10-x}H_{16}$. The probability of various structures appearing within $Si_xGe_{10-x}H_{16}$ nanocrystals depends on temperature and chemical potential environment. The influence of vibrational free energy, as investigated by theoretical computations, is also summarized. The research results show that vibrational free energy enhances the structure stability by the occupation of Ge atoms and results in a more concentrated distribution of the gap between the highest occupied molecular orbital and the lowest unoccupied molecular orbital.

1. Introduction

Nanocrystals have become one of the preferred materials for controlling quantum phenomena at the nanoscale level. The quantum confinement effect allows the luminescent properties of nanocrystals to be tuned by size [1–4]. Such control has brought remarkable performance and extensive applications in the fields of solar cells [5], light emitters [6,7], field-effect transistors [8], and nanosensors [9,10].

Alloying is a practical method for adjusting the properties of materials and exploring novel materials. Due to similar lattice constants in bulk silicon and germanium, spontaneously ordered Si_xGe_{1-x} alloys have been observed in epitaxial growth [35]. Although alloying makes the system more complex, it also provides more opportunities to improving the properties of nanocrystal materials. As silicon-germanium nanocrystal is an infinite solid solution system, the internal atomic distribution within nanocrystal is very complex. Both theory and experiment show that: silicon-germanium nanocrystal exhibit stronger quantum confinement effects than pure silicon nanocrystal and have the advantage of fine-tuning the band gap by changing the atomic ratio of germanium [11–15]. They are also nontoxic, exhibit good biocompatibility and biodegradability, and possess stable chemical properties [16–18].

Structure prediction is essential in many fields of computational science, from molecular physics and biochemistry to soft matter and condensed matter. First-principles calculations can effectively predict the stability and properties of materials at zero temperature. The total energy of Silicon-Germanium nanocrystals can be estimated through a bond energy model, where silicon atoms tend to replace germanium atoms that have a greater number of adjacent hydrogen atoms, followed by a preference for germanium atoms with a greater number of adjacent silicon atoms [19]. The luminescence properties of nanocrystals can be evaluated as the gap between the highest occupied molecular orbital and the lowest unoccupied molecular orbital (HLG) [20,15].

The structure of nanoparticles depends on their size, chemical composition, order, and external conditions such as synthesis method, pressure, temperature, support, etc. At a finite temperature, nanoparticles can transform between different structures. In atomic nanoparticles, temperature can play an important role and entropy becomes important for the contribution of the free energy of individual configurations [21–23]. Experiments show that the Si:Ge ratio and annealing temperature will significantly affect the structure of the synthesized nanocrystals, and the Si/Ge content within the nanocrystals is related to the annealing temperature [24]. Typically, as the free energy is a function of temperature, the atomic distribution in alloy structures will evolve with changing environmental conditions [25]. Recently, it has been proposed to directly calculate the free energy during the global optimization process, providing a promising program for exploring energy landscapes [26].

In this study, in order to take into account the temperature and chemical potential environment while ensuring the accuracy of the calculations when studying the stability and electronic properties of Silicon-

* Corresponding author.
E-mail address: qiushaobin@jyu.edu.cn (S.-B. Qiu).

https://doi.org/10.1016/j.physleta.2024.129793
Received 14 June 2024; Received in revised form 29 July 2024; Accepted 13 August 2024
Available online 22 August 2024

Germanium nanocrystals, we chose the smallest unit $Si_xGe_{10-x}H_{16}$ as the research object as a case study. The number of hydrogen atoms selected here is 16 to ensure the surface passivation of the nanocrystal, which is a common method to stabilize the structure and prevent surface dangling bonds. This choice is consistent with previous studies on similar systems. We perform high-precision first-principles calculations for all $Si_xGe_{10-x}H_{16}$ structures to obtain the energies, HLGs, and frequencies. To describe the stability of $Si_xGe_{10-x}H_{16}$ structures in different chemical potential environments and temperatures, we use the semi-grand canonical ensemble method to calculate the probability of each structure occurring. This ensemble corresponds to the case where the system exchanges particles with reservoirs, which may be fictitious, thus controlling size or composition at a fixed temperature. This approach allows us to identify particularly stable components in multicomponent nanoalloys as the temperature increases and to study the temperature-dependent changes in the properties of material [27,28]. We also considered the influence of vibrational entropy on structural stability. By studying silicon-germanium nanocrystals, this can effectively accelerate their application in modern semiconductor industry, information industry, new energy, biomedical, and other fields.

2. Computational methods

Based on the density functional theory (DFT) method implemented in the Vienna ab initio simulation package (VASP) [29,30], we performed the first-principles calculations on $Si_xGe_{10-x}H_{16}$ nanocrystals. The Perdew-Burke-Ernzerhof generalized gradient approximation (GGA) is applied [31,32]. The cutoff energy is set to 500 eV, and a $1\times1\times1$ grid point is used in the Brillouin zone of the reciprocal lattice. All structures are fully optimized and relaxed using the conjugate gradient method until the force on each atom is less than 0.01 eV/Å. To avoid interactions caused by periodic boundary conditions, we use crystal cells with vacuum distances greater than 10 Å to ensure the accuracy of the calculations. We used VASP to calculate the second-order derivative of the total energy with respect to the ion position using the finite difference method, construct the dynamic matrix and diagonalize it to obtain the intrinsic vibrational modes and frequencies of the system. Among the $3N$ modes calculated, the frequencies of 6 modes are essentially zero due to the translational and rotational invariance of the isolated system, and these modes were removed in our subsequent calculations.

To study the stability and electronic properties of silicon-germanium nanocrystals at different proportions, we need to know the atomic distribution of silicon-germanium nanocrystals at different concentrations. The total number of structures is 1024, and due to the combinatorial nature of alloying, the number of structures grows rapidly with the increase in the number of Si atoms. Structural recognition helps avoid many redundant calculations of the same isomers. Using the package of Structures of Alloys Generation And Recognition (SAGAR) [33], we provide the total number of inequivalent structures for various concentrations of nanocrystals in Table 1. There are 90 unique structures found in 1024 possible candidates.

Here, we use the harmonic approximation to calculate the free energy. In practice, the harmonic approximation requires calculating the vibrational frequencies of local minima, which involves constructing and diagonalizing the dynamical matrix (mass-weighted Hessian). The energy of the particles in the harmonic approximation is given by [34]:

$$E = \phi_0 + \sum_{i=1}^{3N} \hbar\omega_i(n_i + \frac{1}{2}), n_i = 0, 1, 2, \cdots \tag{1}$$

Where ϕ_0 is the interaction energy between atoms when all atoms are at equilibrium positions, ω_i is the i-th characteristic frequency of the particle. n_i is the quantum number describing the i-th harmonic mode. The partition function of the grand canonical ensemble of the equilibrium system is:

Table 1
The number of inequivalent structures of $Si_xGe_{10-x}H_{16}$.

x	0	1	2	3	4	5	6	7	8	9	10
n	1	2	5	11	17	18	17	11	5	2	1

$$\Xi(\mu, V, T) = \sum_N e^{\beta\mu N} Z(N, V, T) \tag{2}$$

$$Z(N, V, T) = \sum_\alpha n_\alpha Z_\alpha(N, V, T) \tag{3}$$

Where $\beta = 1/k_BT$, k_B is the Boltzmann constant, N is the number of atoms, μ is the chemical potential corresponding to the atoms. The equilibrium proportions of atoms at a given temperature T depend on the externally imposed chemical potentials μ for each element. For a two-element system, the only relevant parameter is the difference between the assigned chemical potentials, here it's $\Delta\mu = \mu_{Si} - \mu_{Ge}$. n_α is the structural multiplicity caused by the symmetry of the structure. $Z(N, V, T)$ is the partition function of the canonical ensemble:

$$Z_\alpha(N, V, T) = \sum_{\{n_i\}} e^{-\beta E} = e^{-\beta\phi_0} \prod \frac{e^{-\frac{\beta\hbar\omega_i}{2}}}{1 - e^{-\beta\hbar\omega_i}} \tag{4}$$

The occupation probability of a nonequivalent structure can be written as:

$$p_\alpha = \frac{n_\alpha e^{\beta\mu N} Z_\alpha(N, V, T)}{\Xi(\mu, V, T)} \tag{5}$$

3. Results and discussions

In hydrogen passivated silicon-germanium nanocrystals, all sites occupied by Si/Ge atoms can be divided into three categories: site connected with 0 hydrogen atoms (type A site), site connected with 1 hydrogen atom (type B sites) and site connected by 2 hydrogen atom (type C site). Each type C site is separated by type A and type B sites. Analysis reveals that the stability of the structure is related to the type of site where the silicon and germanium atoms are located. In previous studies, we found that Si atoms tend to occupy sites with more connected hydrogen atoms, followed by sites with more neighboring Si atoms [19]. $Si_{10}H_{16}$ and $Ge_{10}H_{16}$ have high symmetry, with 24 symmetry operations. It's a cage-like molecule surrounded by 6 type C sites 4 type B sites, as shown in Fig. 1(a). Due to symmetry, four type B sites are equivalent, and six type A sites are also equivalent.

Through first-principles calculations, we got the total energy of $Si_xGe_{10-x}H_{16}$. Because of the different chemical compositions between structures, in order to compare their relative stability without considering the influence of chemical potential changes, we first compare the structures with different doping conditions of the same cluster structure. Here, we use the formation enthalpy to describe the relative stability of the structures. The reference phases for $Si_xGe_{10-x}H_{16}$ are $Si_{10}H_{16}$ and $Ge_{10}H_{16}$. Therefore, the formula for calculating the formation enthalpy ΔH is:

$$\Delta H_i = E_i - \frac{\left[xE_{Si_{10}H_{16}} + (10-x)E_{Ge_{10}H_{16}}\right]}{10}, \tag{6}$$

where E_i, $E_{Si_{10}H_{16}}$, and $E_{Ge_{10}H_{16}}$ are the total energies of the i-th $Si_xGe_{10-x}H_{16}$, $Si_{10}H_{16}$, and $Ge_{10}H_{16}$, respectively.

The formation enthalpy of $Si_xGe_{10-x}H_{16}$ is shown in Fig. 1(b). Under each concentration of $Si_xGe_{10-x}H_{16}$, some structures have formation energies less than or equal to 0, indicating that $Si_xGe_{10-x}H_{16}$ is not phase-separated system. The lowest formation energy is -0.224 eV, corresponding to the most stable structure $Si_6Ge_4H_{16}$. Si atoms tend to occupy sites with more connected hydrogen atoms, followed by sites with more neighboring Si atoms. The lowest points of formation enthalpy for $x = 0 \sim 6$ linearly change with the number of Si atoms, with the energy difference between the adjacent lowest points being approximately 0.036 eV. Similarly, the lowest points of formation enthalpy for

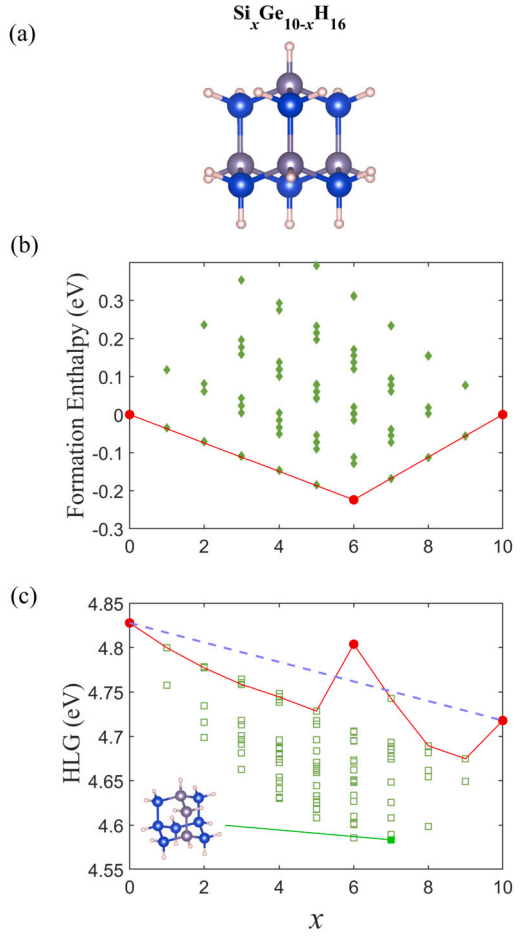

Fig. 1. (a) Structure of $Si_xGe_{10-x}H_{16}$, where pink spheres represent H atoms, and Si and Ge atoms are represented by blue spheres and gray spheres, respectively. (b) Formation enthalpy of $Si_xGe_{10-x}H_{16}$ is represented by a green solid prism, and the convex hull points are represented by red circles. (c) HLGs of $Si_xGe_{10-x}H_{16}$. The HLGs corresponding to the most stable structure at each concentration are connected by a solid red line.

$x = 6 \sim 10$ also change linearly with the number of Si atoms, with the energy difference between the adjacent lowest points being approximately 0.056 eV.

We show the HLGs of $Si_xGe_{10-x}H_{16}$ in Fig. 1(c). The distribution of HLGs ranges from 4.58 to 4.83 eV. The largest HLG is for $Ge_{10}H_{16}$ without Si doping, reaching 4.828 eV, and $Si_{10}H_{16}$ has an HLG of 4.718 eV, smaller than that of $Ge_{10}H_{16}$. The structure $Si_7Ge_3H_{16}$ with the lowest HLG is given in the inserted plot. The structure $Si_6Ge_4H_{16}$ with the lowest formation enthalpy has the largest HLG among intermediate concentration structures, with a value of 4.804 eV.

Using the semi-grand canonical ensemble method, we can calculate the expected value of the fraction of silicon and germanium atoms in different chemical potential environments. Using Eq. (2), we obtain the relationship between the proportion of Si atoms in $Si_xGe_{10-x}H_{16}$ and the chemical potential difference ($\Delta\mu$) between Si and Ge in Fig. 2. It can be seen that the proportion of Si atoms is monotonically changing with $\Delta\mu$ when the temperature is constant, so a $\Delta\mu$ can correspond to a unique expected value of the proportion. Similarly, when we want to study the system under a certain particle ratio, we just need to use Eq. (2) and substitute the $\Delta\mu$ value corresponding to the particle ratio into the equation. In the nanocrystal, the concentration of Si atoms increases with the increase of $\Delta\mu$. At low temperatures, the range of $\Delta\mu$ corresponding to concentrations 0 to 1 is relatively small. As the temperature increases, this range will gradually expand. For the case without considering vibrational entropy, as shown in Fig. 2(a), when T = 50 K, the range of

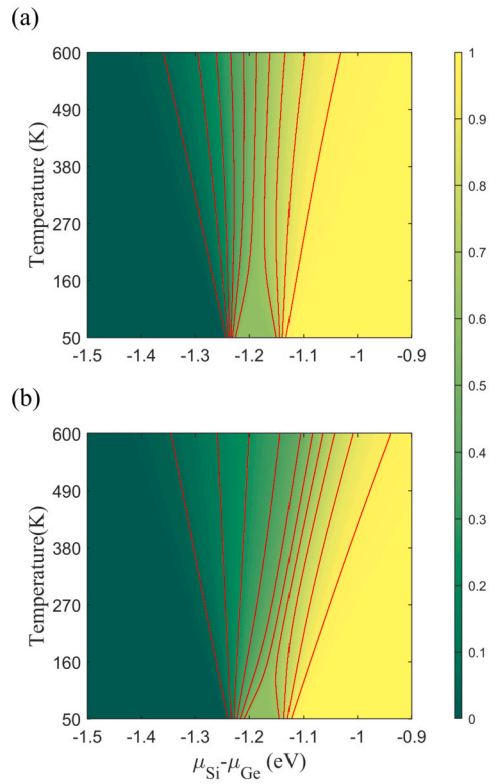

Fig. 2. The proportion of Si atoms in $Si_xGe_{10-x}H_{16}$ nanocrystals with different chemical potential environments and temperatures. (a) Results of only considering configurational entropy. (b) Results of considering both configurational entropy and vibrational entropy.

$\Delta\mu$ corresponding to the variation of Si atom concentration from 0.1 to 0.9 is -1.24 to 1.14 eV, and T = 500 K, it is -1.30 to 1.09 eV. For the case considering both configurational entropy and vibrational entropy, as shown in Fig. 2(b). When T = 50 K, the range of $\Delta\mu$ corresponding to the variation of Si atom concentration from 0.1-0.9 is -1.23 to 1.13 eV. And T = 500 K, it is -1.28 to 1.01 eV. Comparing the two cases, we find that at low temperatures, $\Delta\mu$ range corresponding to the variation of Si atom concentration from 0.1 to 0.9 is basically the same for both cases. As the temperature increases, the rate at which the $\Delta\mu$ range expands is faster for the latter case than for the former case, and the $\Delta\mu$ range moves in the direction of increasing values. Therefore, we can see that if only the configurational entropy is considered, the chemical potential corresponding to Si concentration equal to 0.5 hardly changes with temperature. However, if both configurational entropy and vibrational entropy are considered, the chemical potential corresponding to a Si concentration of 0.5 will increase with temperature increases.

The relationships between the concentration of Si atoms occupied at the type B(type C) sites and the total concentration of Si(x) in the nanocrystal are showed in Figs. 3(a) and 3(c). At a low temperature of 50 K, the curves considering the vibration entropy and ignoring it are completely overlapped. It can be clearly seen that as x increases, the Si concentration at type B sites begins to rise linearly after the type C sites are fully occupied. When the temperature reaches 500 K, the curves considering vibration entropy and ignoring it are no longer completely overlapped, but the overall trend is the same: when x is small, the number at type C sites mainly increases, and the curve of type B sites increases very slowly. When the total concentration is large, the curve of type C sites increases slowly, and curve of type B sites increases faster. In the case of vibration entropy, it is found that the concentration at type B sites increases significantly when x is small.

The relationships between the concentration of Si atom at type B(type C) sites and the chemical potential in the nanocrystal are showed

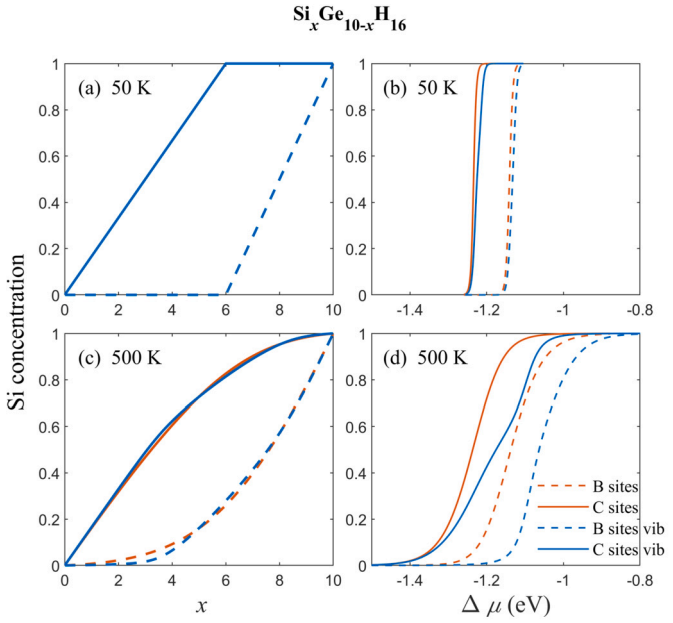

Fig. 3. The variation of concentration at the type B(type C) sites. (a)(b) When $T = 50$ K, variation of concentration at the type B(type C) sites with total concentration of Si(x) and chemical potential in the nanocrystal. (c)(d) The situation at a temperature of 500 K.

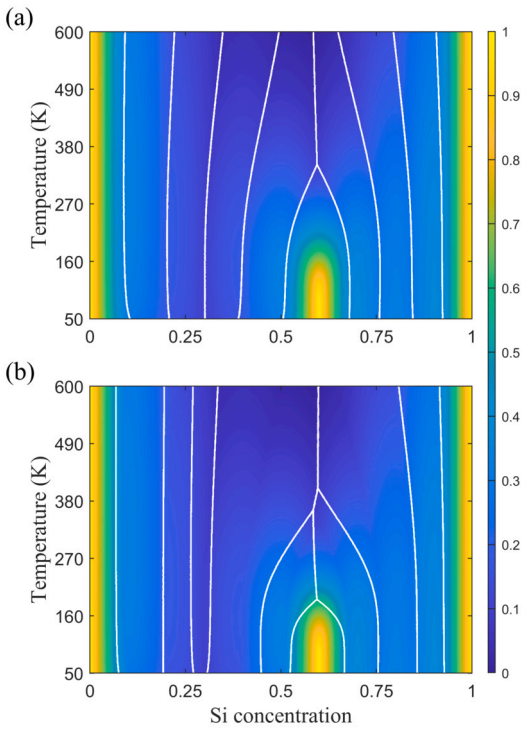

Fig. 4. The most stable structures of $Si_xGe_{16-x}H_{16}$ and their probabilities of occurrence with respect to concentration of Si and temperature. (a) Results of only considering configurational entropy. (b) Results of considering both configurational entropy and vibrational entropy.

in Figs. 3(b) and 3(d). When $T = 50$ K, the concentration at both type B and type C sites increases rapidly to the maximum value after the chemical potential reaches a certain value. Without considering the vibrational entropy, the point of inflection of the curve at type B sites is around $\Delta\mu = -1.14$ eV, and the point of type C sites is around $\Delta\mu = -1.23$ eV, with a difference of 0.09 eV. These two values correspond exactly to the change in total energy ΔE when a Si atom replaces a Ge atom in $Si_xGe_yH_z$ at sites C1 and B4 in previous work [19]. The vibrational entropy moves the point of inflection in the direction of increasing $\Delta\mu$. When the temperature increases to 500 K, the concentration increases more slowly with the chemical potential. Without considering the vibrational entropy, the spacing between the concentration curves of type B and type C sites remains at around 0.09 eV. Compared with the low-temperature case, the concentration begins to increase at a smaller chemical potential. However, to reach the full occupation number, the corresponding chemical potential needs to be higher. Additionally, after considering the vibration entropy, when the concentration of type B sites begins to increase significantly, the corresponding chemical potential is higher.

We compared the most stable structures of $Si_xGe_{16-x}H_{16}$ and their probabilities of occurrence with respect to the concentration of Si and temperature, as shown in Fig. 4. Fig. 4 (a) represents the cases of not considering vibrational entropy, and the figure is divided into 10 sections by white solid lines. $Si_6Ge_4H_{16}$ as the lowest formation enthalpy structure, which corresponds to the candle-shaped region around a Si atom proportion of 0.6 in Fig. 4 (a). It is found that when the concentration is around 0.6 and temperature under 180 K, the probability of occurrence of this structure is very high. As the temperature increases, the occupation probability of $Si_6Ge_4H_{16}$ remains the highest, but the probability decreases, indicating that the system is approaching a mixed state of multiple structures. Experimental results show that nanocrystals formed at high temperatures are more polycrystalline than films annealed at 700 °C and 800 °C [24]. This is consistent with our calculations. The region corresponding to this structure gradually narrows as the temperature rises until it is merged by structures on both sides at 350 K and the most dominant position is replaced. The occupation probability of the most stable structure near concentration of Si is 0.3, corresponding to $Si_3Ge_7H_{16}$, is very low. And the region corresponding to $Si_6Ge_4H_{16}$ gradually narrows with the increase in temperature because of the high symmetry of these two structures, resulting in a low multiplicity of structures. In fact, in the areas close to dark blue, the proportion of each structure is relatively small. Fig. 4 (b) presents the results considering the vibrational entropy. The figure is divided into 11 sections by white solid lines, corresponding to the 11 most stable structures with Si atom numbers ranging from 0 to 10. Similarly to the situation in Fig. 4 (a), $Si_6Ge_4H_{16}$ corresponds to the candle-shaped region around a Si atom proportion of 0.6 in Fig. 4 (b). It is merged by structures on both sides and replaced at the most dominant position at 180 K, earlier compared to when vibrational entropy is not considered.

The distribution of HLG depends on the occupation probability. Fig. 5 presents the distribution of HLGs for silicon atom concentrations of 0.4 and 0.6. At low temperatures, the structures with small formation energy are generally dominant, resulting in the peak of the probability occurs at their corresponding HLG. As the temperature increases, the probabilities of HLGs corresponding to other structures also increase. When $n = 0.4$, the distribution of HLG at low temperature is concentrated between 4.73 eV and 4.80 eV. At 600 K, the distribution range of HLG is significantly expanded, but several peaks are still concentrated in the low-temperature range. In both cases, considering vibration entropy will make the distribution of HLG more concentrated. When $n = 0.6$, the most stable structure in the ground state is $Si_6Ge_4H_{16}$, so there is only a peak corresponding to its HLG at low temperature. At 600 K, the distribution of HLG is very scattered, but the HLG of $Si_6Ge_4H_{16}$ is still one of the higher peaks. However, it can be seen that considering vibration entropy will significantly reduce the peak height of $Si_6Ge_4H_{16}$.

4. Conclusions

In summary, we used first-principles calculations to obtain the ground-state energies and electronic properties of all possible structures of $Si_xGe_{16-x}H_{16}$ nanocrystals. We used ensemble theory to analyze $Si_xGe_{16-x}H_{16}$ at finite temperature and determined the correspondence

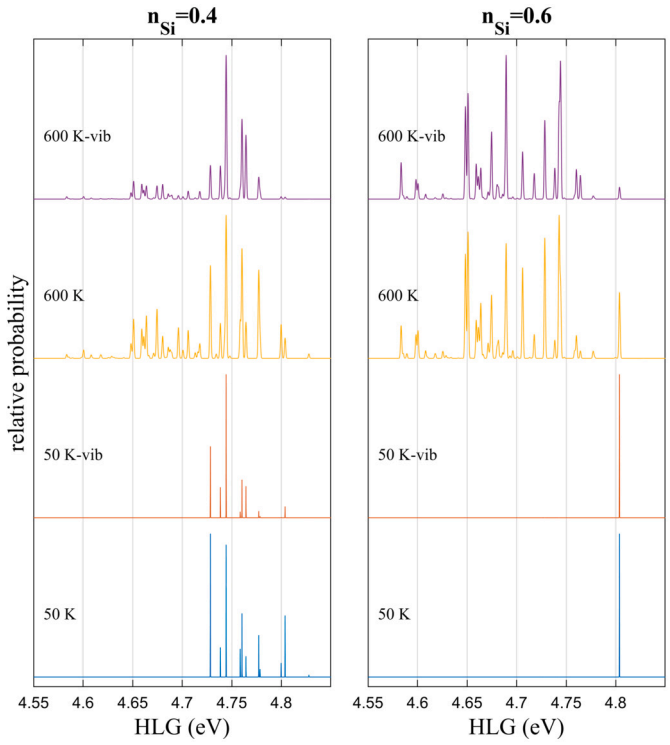

Fig. 5. The probability of HLG distribution for $Si_xGe_{16-x}H_{16}$.

between chemical potential environments and atomic occupancy at different temperatures. By studying the probability of various structures in $Si_xGe_{16-x}H_{16}$ under temperature and chemical potential environments, we analyzed the changes in stability and properties at different temperatures. At the same time, we also considered the effect of vibrational free energy on stability and found that vibrational free energy makes the stability of the structure closer to the occupancy of Ge atoms. Vibrational free energy will significantly affect the probability distribution of HLG, so it is very necessary to take it into account during the research process. Our results show that by analyzing the temperature effect more systematically and accurately, we can obtain the stability and properties of nanocrystals that are closer to the actual situation, further strengthening the role of theoretical calculations in nanocrystal research.

CRediT authorship contribution statement

Shao-Bin Qiu: Writing – review & editing, Writing – original draft, Visualization, Software, Resources, Methodology, Investigation, Data curation, Conceptualization. **Dan-Feng Zhu:** Writing – review & editing, Visualization. **Ding-Nan Deng:** Writing – review & editing. **Jun-Bo Chen:** Writing – review & editing. **Yu-Jun Zhao:** Writing – review & editing, Software, Conceptualization. **Xiao-Bao Yang:** Writing – review & editing, Supervision, Software, Methodology, Investigation, Conceptualization.

Declaration of competing interest

The authors declare that they have no known competing financial interests or personal relationships that could have appeared to influence the work reported in this paper.

Data availability

Data will be made available on request.

Acknowledgements

This work was supported by Talented Research Start-up Project of Jiaying University (2022RC09, 2022RC10, 2022RC11), 2023 Science and Technology Project of Jiaying University(2023KJY15, 2023KJY17), Meizhou City Social Development Science and Technology Plan Project (2021B127).

References

[1] J.M. Pietryga, Y.-S. Park, J. Lim, A.F. Fidler, W.K. Bae, S. Brovelli, V.I. Klimov, Spectroscopic and device aspects of nanocrystal quantum dots, Chem. Rev. 116 (18) (2016) 10513–10622.
[2] M.A. Boles, D. Ling, T. Hyeon, D.V. Talapin, The surface science of nanocrystals, Nat. Mater. 15 (2) (2016) 141–153.
[3] M.V. Kovalenko, L. Manna, A. Cabot, Z. Hens, D.V. Talapin, C.R. Kagan, V.I. Klimov, A.L. Rogach, P. Reiss, D.J. Milliron, P. Guyot-Sionnnest, G. Konstantatos, W.J. Parak, T. Hyeon, B.A. Korgel, C.B. Murray, W. Heiss, Prospects of nanoscience with nanocrystals, ACS Nano 9 (2) (2015) 1012–1057.
[4] A.L. Efros, L.E. Brus, Nanocrystal quantum dots: from discovery to modern development, ACS Nano 15 (4) (2021) 6192–6210.
[5] D. Carolan, Recent advances in germanium nanocrystals: synthesis, optical properties and applications, Prog. Mater. Sci. 90 (2017) 128–158.
[6] A.-M. Lepadatu, I. Stavarache, A. Maraloiu, C. Palade, T.V. Serban, C.L. Magdalena, Electrical behaviour related to structure of nanostructured GeSi films annealed at 700 °C, in: CAS 2012 (International Semiconductor Conference), IEEE, 2012, pp. 109–112.
[7] E.M.F. Vieira, J. Toudert, A.G. Rolo, A. Parisini, J.P. Leitão, M.R. Correia, N. Franco, E. Alves, A. Chahboun, J. Martín-Sánchez, R. Serna, M.J.M. Gomes, SiGe layer thickness effect on the structural and optical properties of well-organized SiGe/SiO2 multilayers, Nanotechnology 28 (34) (2017) 345701.
[8] Y. Cui, Z. Zhong, D. Wang, W.U. Wang, C.M. Lieber, High performance silicon nanowire field effect transistors, Nano Lett. 3 (2) (2003) 149–152.
[9] A.-M. Lepadatu, I. Stavarache, C. Palade, A. Slav, I. Dascalescu, O. Cojocaru, V.-A. Maraloiu, V.S. Teodorescu, T. Stoica, M.L. Ciurea, Enhancing short-wave infrared photosensitivity of SiGe nanocrystals-based films through embedding matrix-induced passivation, stress, and nanocrystallization, J. Phys. Chem. C 128 (10) (2024) 4119–4142.
[10] C. Palade, I. Stavarache, T. Stoica, M.L. Ciurea, GeSi nanocrystals photo-sensors for optical detection of slippery road conditions combining two classification algorithms, Sensors 20 (21) (2020).
[11] M.S. Uddin, S. Khatun, C. Vijayan, J. Rath, Bandgap study of quantum dot-sized SiGe alloy nanocrystals prepared in a nonthermal capacitively-coupled plasma by ambient scanning tunneling spectroscopy, Phys. Rev. B, Condens. Matter 675 (2024) 415625.
[12] S. Pan, B. Zhou, S. Chen, C. Li, W. Huang, H. Lai, Optical property investigation of SiGe nanocrystals formed by electrochemical anodization, Appl. Surf. Sci. 258 (1) (2011) 30–33.
[13] E. Tuğay, S. Ilday, R. Turan, T.G. Finstad, Influence of Ge content and annealing conditions on the PL properties of nc-Si1-xGex embedded in SiO2 matrix in weak quantum confined regime, J. Lumin. 155 (2014) 170–179.
[14] S. Takeoka, K. Toshikiyo, M. Fujii, S. Hayashi, K. Yamamoto, Photoluminescence from $Si_{1-x}Ge_x$ alloy nanocrystals, Phys. Rev. B 61 (23) (2000) 15988–15992.
[15] O. Cojocaru, A.-M. Lepadatu, G. Nemnes, T. Stoica, M. Ciurea, Bandgap atomistic calculations on hydrogen-passivated GeSi nanocrystals, Sci. Rep. 11 (2021) 13582.
[16] N.H. Alsharif, C.E.M. Berger, S.S. Varanasi, Y. Chao, B.R. Horrocks, H.K. Datta, Alkyl-capped silicon nanocrystals lack cytotoxicity and have enhanced intracellular accumulation in malignant cells via cholesterol-dependent endocytosis, Small 5 (2) (2009) 221–228.
[17] P.O. Anikeeva, J.E. Halpert, M.G. Bawendi, V. Bulović, Quantum dot light-emitting devices with electroluminescence tunable over the entire visible spectrum, Nano Lett. 9 (7) (2009) 2532–2536.
[18] J.-H. Park, L. Gu, G. von Maltzahn, E. Ruoslahti, S. Bhatia, M. Sailor, Biodegradable luminescent porous silicon nanoparticles for in vivo applications, Nat. Mater. 8 (4) (2009) 331–336.
[19] S.-B. Qiu, Y.-T. Wang, C.-C. He, X.-L. Deng, X.-B. Yang, Structural stabilities and optical properties of sixgeyhz nanocrystals, Phys. Lett. A 384 (25) (2020) 126597.
[20] K. Dohnalová, A.N. Poddubny, A. Prokofiev, W.D.A.M. de Boer, C.P. Umesh, J.M.J. Paulusse, H. Zuilhof, T. Gregorkiewicz, Surface brightens up Si quantum dots: direct bandgap-like size-tunable emission, Light: Sci. Appl. 2 (1) (2013) e47.
[21] J. Kim, B.J. Mhin, S.J. Lee, K.S. Kim, Entropy-driven structures of the water octamer, Chem. Phys. Lett. 219 (3) (1994) 243–246.
[22] J.P.K. Doye, F. Calvo, Entropic effects on the structure of Lennard-Jones clusters, J. Chem. Phys. 116 (19) (2002) 8307–8317.
[23] A.A. Nickson, K.E. Stoll, J. Clarke, Folding of a lysm domain: entropy-enthalpy compensation in the transition state of an ideal two-state folder, J. Mol. Biol. 380 (3) (2008) 557–569.
[24] I. Stavarache, C. Logofatu, M.T. Sultan, A. Manolescu, H.G. Svavarsson, V.S. Teodorescu, M.L. Ciurea, SiGe nanocrystals in SiO2 with high photosensitivity from visible to short-wave infrared, Sci. Rep. 10 (1) (2020) 3252.

[25] F. Calvo, D. Schebarchov, D.J. Wales, Grand and semigrand canonical basin-hopping, J. Chem. Theory Comput. 12 (2) (2016) 902–909, pMID: 26669731.
[26] K. Sutherland-Cash, D. Wales, D. Chakrabarti, Free energy basin-hopping, Chem. Phys. Lett. 625 (2015) 1–4.
[27] J. Weinreich, M.L. Paleico, J. Behler, Properties of α-brass nanoparticles II: structure and composition, J. Phys. Chem. C 125 (27) (2021) 14897–14909.
[28] F. Baletto, Structural properties of sub-nanometer metallic clusters, J. Phys. Condens. Matter 31 (11) (2019) 113001.
[29] G. Kresse, J. Furthmüller, Efficient iterative schemes for ab initio total-energy calculations using a plane-wave basis set, Phys. Rev. B 54 (1996) 11169–11186.
[30] G. Kresse, D. Joubert, From ultrasoft pseudopotentials to the projector augmented-wave method, Phys. Rev. B 59 (1999) 1758–1775.
[31] J.P. Perdew, K. Burke, M. Ernzerhof, Generalized gradient approximation made simple, Phys. Rev. Lett. 77 (1996) 3865–3868.
[32] J.P. Perdew, K. Burke, M. Ernzerhof, Perdew, Burke, and Ernzerhof reply, Phys. Rev. Lett. 80 (1998) 891.
[33] C.-C. He, J.-H. Liao, S.-B. Qiu, Y.-J. Zhao, X.-B. Yang, Biased screening for multi-component materials with structures of alloy generation and recognition (sagar), Comput. Mater. Sci. 193 (2021) 110386.
[34] F. Calvo, D. Wales, Harmonic superposition method for grand-canonical ensembles, Chem. Phys. Lett. 623 (2015) 17–21.
[35] G. Katsaros, P. Spathis, M. Stoffel, F. Fournel, M. Mongillo, V. Bouchiat, F. Lefloch, A. Rastelli, O.G. Schmidt, S. De Franceschi, Hybrid superconductor–semiconductor devices made from self-assembled SiGe nanocrystals on silicon, Nat. Nanotechnol. 5 (6) (2010) 458–464.